A

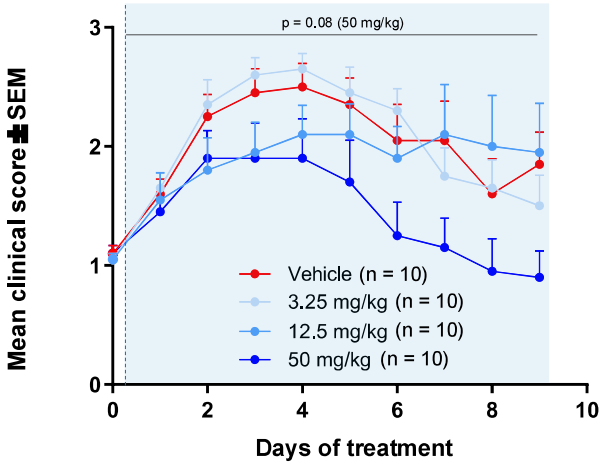
p = 0.08 (50 mg/kg)
Mean clinical score ± SEM
Vehicle (n = 10)
3.25 mg/kg (n = 10)
12.5 mg/kg (n = 10)
50 mg/kg (n = 10)
Days of treatment

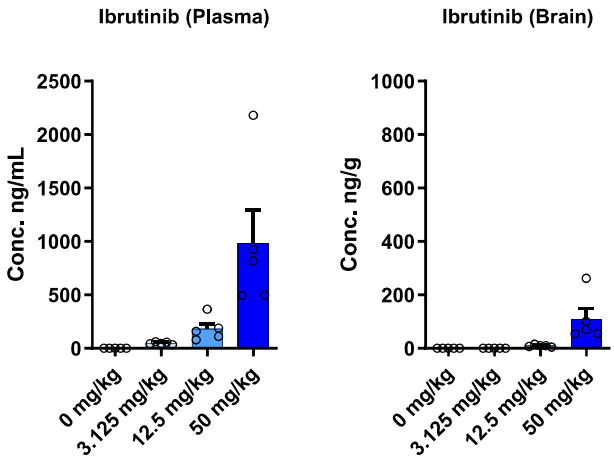
Ibrutinib (Plasma)
Conc. ng/mL
0 mg/kg
3.125 mg/kg
12.5 mg/kg
50 mg/kg
Ibrutinib (Brain)
Conc. ng/g

B

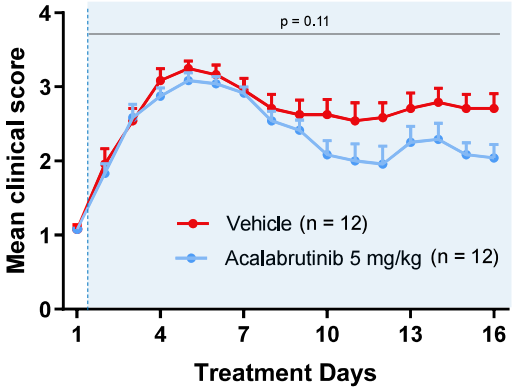
p = 0.11
Mean clinical score
Vehicle (n = 12)
Acalabrutinib 5 mg/kg (n = 12)
Treatment Days

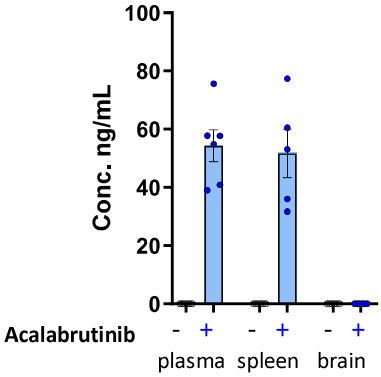
Conc. ng/mL
Acalabrutinib
plasma
spleen
brain

Fig. S1. Non-CNS-penetrant BTK inhibition in the C57BL/6 EAE mouse model of MS. (A) Disease scores over time in mice treated with BTK inhibitor ibrutinib and respective end-of-study inhibitor concentrations in plasma and brain, one hour post final dose. (B) Disease scores over time in mice treated with BTK inhibitor acalabrutinib and respective end-of-study inhibitor concentrations in plasma and brain, one hour post final dose. Therapeutic treatment started once disease scores initially reach 1.0-1.5 (i.e. treatment from onset). P-values are indicated by *≤0.05, **≤0.01, ***≤0.001, and ****≤0.0001. Source data are provided as a Source Data file.

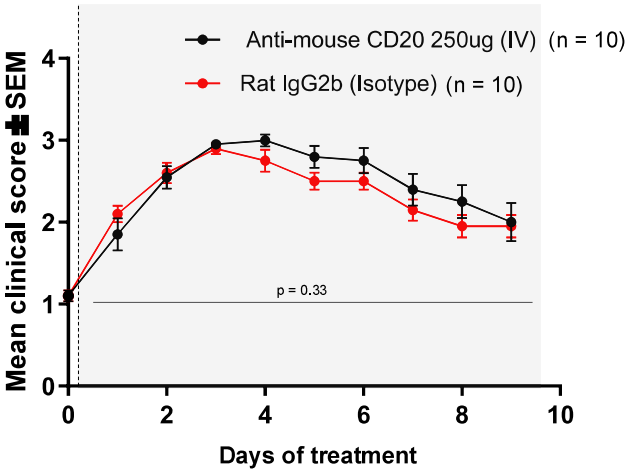
Anti-mouse CD20 250ug (IV) (n = 10)
Rat IgG2b (Isotype) (n = 10)
Mean clinical score ± SEM
p = 0.33
Days of treatment
0
1
2
3
4
0
2
4
6
8
10

Fig. S2. B cell depletion in the C57BL/6 EAE mouse model of MS. Disease scores over time in mice treated with B cell-depleting anti-CD20 antibodies. Therapeutic treatment started once disease scores reached 1.0-1.5. Source data are provided as a Source Data file.

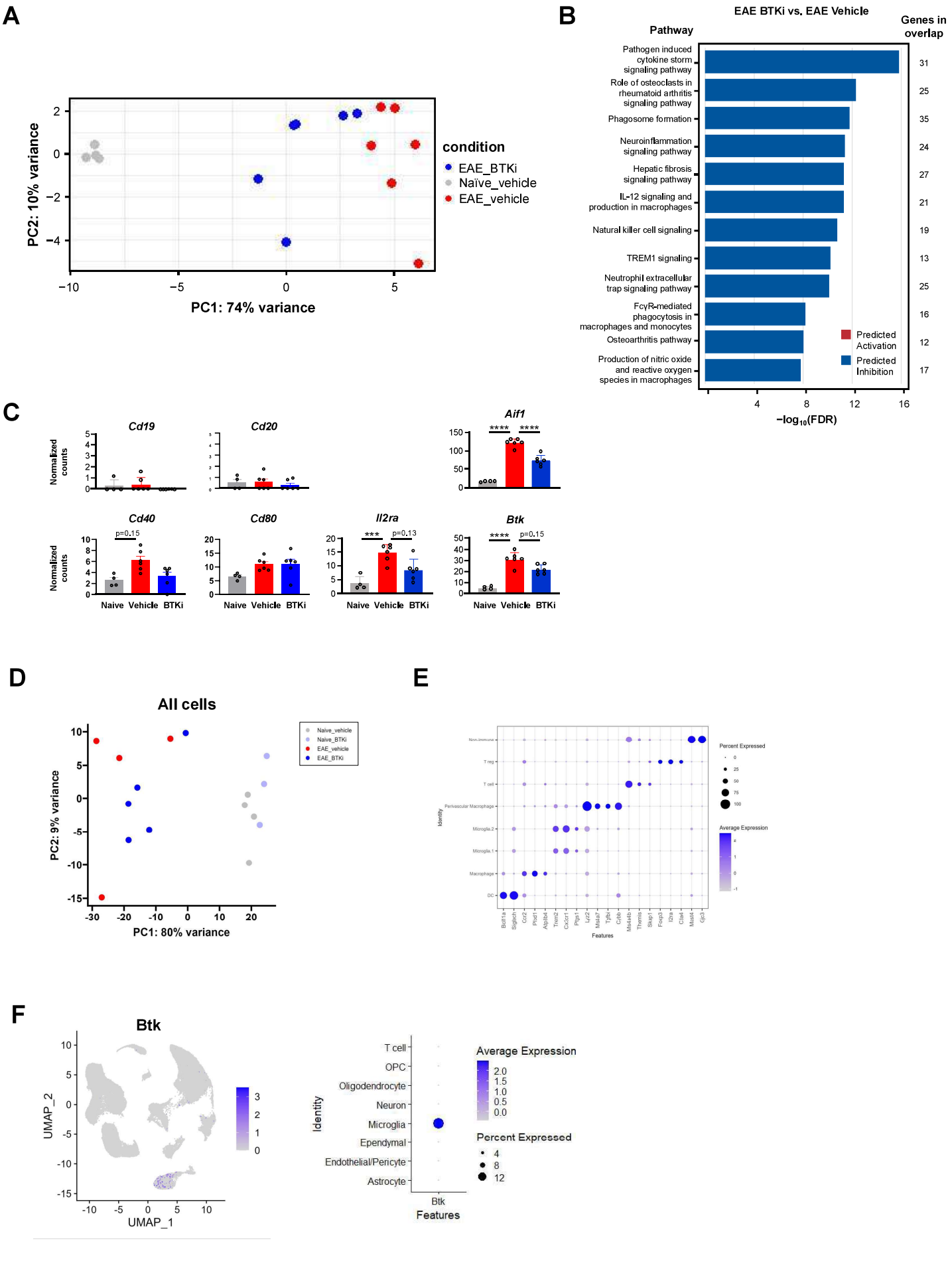
A
PC2: 10% variance
PC1: 74% variance
condition
EAE_BTKi
Naïve_vehicle
EAE_vehicle
B
EAE BTKi vs. EAE Vehicle
Pathway
Genes in overlap
Pathogen induced cytokine storm signaling pathway
Role of osteoclasts in rheumatoid arthritis signaling pathway
Phagosome formation
Neuroinflammation signaling pathway
Hepatic fibrosis signaling pathway
IL-12 signaling and production in macrophages
Natural killer cell signaling
TREM1 signaling
Neutrophil extracellular trap signaling pathway
FcγR-mediated phagocytosis in macrophages and monocytes
Osteoarthritis pathway
Production of nitric oxide and reactive oxygen species in macrophages
31
25
35
24
27
21
19
13
25
16
12
17
Predicted Activation
Predicted Inhibition
−log10(FDR)
C
Cd19
Cd20
Aif1
Cd40
Cd80
Il2ra
Btk
Normalized counts
p=0.15
p=0.13
****
***
Naive
Vehicle
BTKi
D
All cells
PC2: 9% variance
PC1: 80% variance
Naive_vehicle
Naive_BTKi
EAE_vehicle
EAE_BTKi
E
Percent Expressed
Average Expression
Identity
Features
F
Btk
UMAP_2
UMAP_1
T cell
OPC
Oligodendrocyte
Neuron
Microglia
Ependymal
Endothelial/Pericyte
Astrocyte
Average Expression
Percent Expressed
Identity
Features

Fig. S3. EAE-dependent transcriptional response after treatment initiation in the spinal cord of C57BL/6 EAE mice. (A) Principal component analysis (PCA) of bulk RNA sequencing data from EAE mouse spinal cords, shown in Fig. 1C. Variance stabilizing transformed counts from DESeq2 were used for PCA. Profiles of individual animals are shown plotted against the two principal components comprising the greatest variance. (B) IPA pathway analysis of differentially expressed genes identified by bulk RNA sequencing in Fig. 1C. The 12 pathways that demonstrated the largest change ($-\log_{10}$(FDR)) and showed direction (i.e. had a z-score available) are presented. All 12 pathways shown were downregulated with EAE + PRN2675 vs EAE + vehicle. (C) DESeq2 normalized counts of the *Btk* gene and genes encoding markers of T lymphocytes (*Il2ra*), B lymphocytes (*Cd19, Cd20, Cd40, and Cd80*), and microglia/macrophages (*Aif1*), among bulk RNA sequencing dataset described in Fig. 1C. (D) PCA of snRNAseq all cell pseudo-bulk data from EAE mouse spinal cords, shown in Fig. 1D. Variance stabilizing transformed counts from DESeq2 were used. Profiles of individual animals are shown plotted against the two principal components comprising the greatest variance. (E) Dot plot of cell-type markers for immune cell types identified in Fig. 1E. (F) Cellular enrichment of *Btk* expression among the CNS cell-type clusters generated from snRNAseq of EAE mouse spinal cords, shown in Fig. 1D. P-values are indicated by *≤0.05, **≤0.01, ***≤0.001, and ****≤0.0001. BTK = Bruton's tyrosine kinase; BTKi = BTK inhibitor; EAE = experimental autoimmune encephalomyelitis; IL = interleukin; IPA = ingenuity pathway analysis.

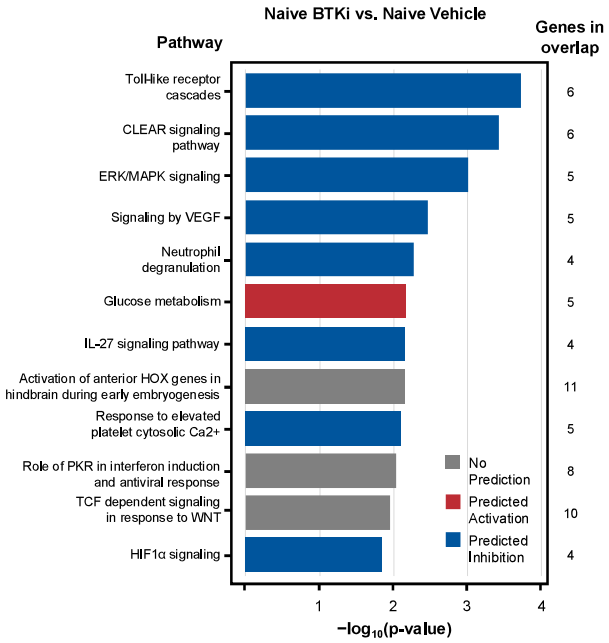
Naive BTKi vs. Naive Vehicle
Pathway
Genes in overlap
Toll-like receptor cascades
CLEAR signaling pathway
ERK/MAPK signaling
Signaling by VEGF
Neutrophil degranulation
Glucose metabolism
IL-27 signaling pathway
Activation of anterior HOX genes in hindbrain during early embryogenesis
Response to elevated platelet cytosolic Ca2+
Role of PKR in interferon induction and antiviral response
TCF dependent signaling in response to WNT
HIF1α signaling
6
6
5
5
4
5
4
11
5
8
10
4
No Prediction
Predicted Activation
Predicted Inhibition
1
2
3
4
−log10(p-value)

Fig. S4. Transcriptional response after treatment initiation in the spinal cord of naive C57BL/6 mice. Pathway analysis using IPA: Naive + PRN2675 vs naive + vehicle. The 12 pathways that demonstrated the largest change ($-\log_{10}$(raw p-value)) and showed direction (i.e. had a z-score available) are presented. The pathway analysis gene list is the PRN2675-dependent transcriptional signature identified in the left plot of Fig. 1G.

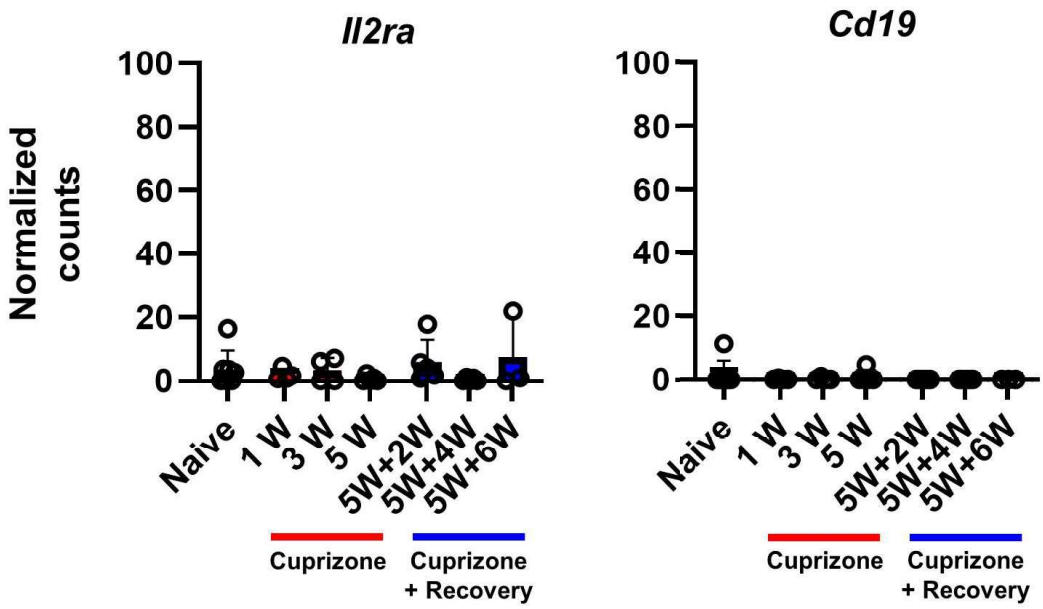
Il2ra
Cd19
Normalized counts
100
80
60
40
20
0
Naive
1 W
3 W
5 W
5W+2W
5W+4W
5W+6W
Cuprizone
Cuprizone + Recovery

Fig. S5. mRNA expression of genes encoding markers of T lymphocytes (*Il2ra*) and B lymphocytes (*Cd19*) in the cuprizone mouse model of demyelination. W = week.

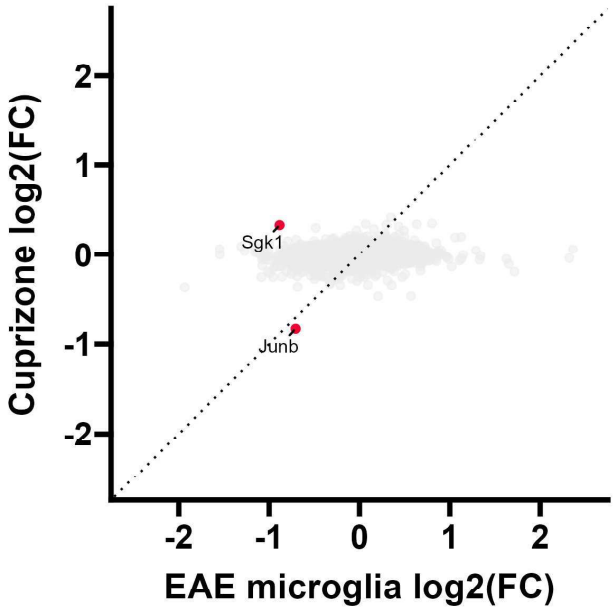
Cuprizone log2(FC)
EAE microglia log2(FC)
Sgk1
Junb
2
1
0
-1
-2
-2
-1
0
1
2

Fig. S6. Genes commonly modulated by BTKi in cuprizone mouse model bulk spinal cord and EAE mouse microglia. Four-way plot of cuprizone bulk spinal cord differential expression results for cuprizone + PRN2675 vs. cuprizone + vehicle (Fig. 2E) and EAE pseudo-bulk microglia differential expression results for EAE + PRN2675 vs EAE + vehicle (Fig. 1G, right). Labelled genes were commonly significantly differentially expressed genes between the two analyses (for EAE microglia, absolute(fold-change) >= 1.5 and raw p-value <= 0.05; for cuprizone bulk, absolute(fold-change) >= 1.2 and raw p-value <= 0.05).

A

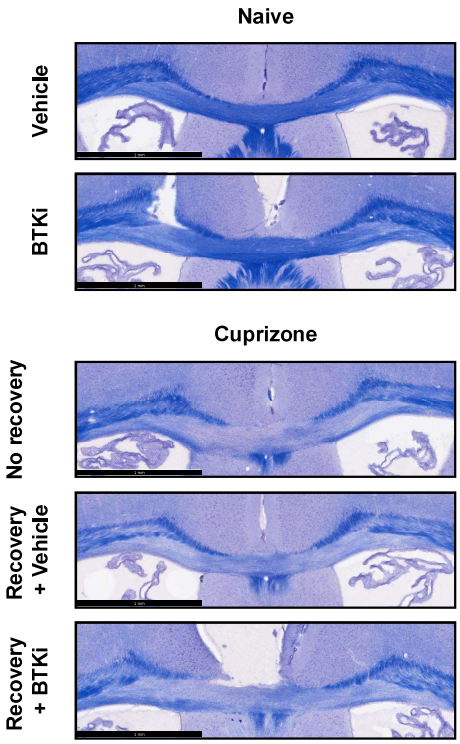
Naive
Vehicle
BTKi
Cuprizone
No recovery
Recovery + Vehicle
Recovery + BTKi

B

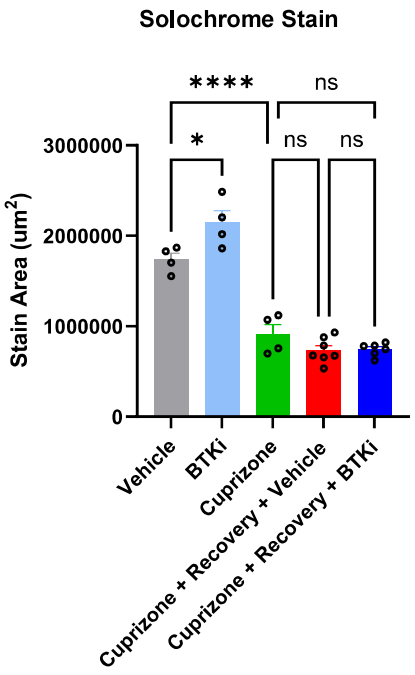
Solochrome Stain
****
ns
*
ns
ns
3000000
2000000
1000000
0
Stain Area (um2)
Vehicle
BTKi
Cuprizone
Cuprizone + Recovery + Vehicle
Cuprizone + Recovery + BTKi

Fig. S7. Effect of BTK-inhibiting tool compound PRN2675 on remyelination in a cuprizone mouse model of demyelination. PRN2675 was administered after 5 weeks of cuprizone treatment and continued for 4 days alongside cuprizone recovery. The cuprizone alone condition denotes 5 weeks of cuprizone with no subsequent recovery period. (A) Solochrome staining for intact myelin in the corpus callosum. (B) Solochrome stain area was measured using HALO. P-values are indicated by *≤0.05, **≤0.01, ***≤0.001, and ****≤0.0001. BTKi = Bruton's tyrosine kinase inhibitor. Source data are provided as a Source Data file.

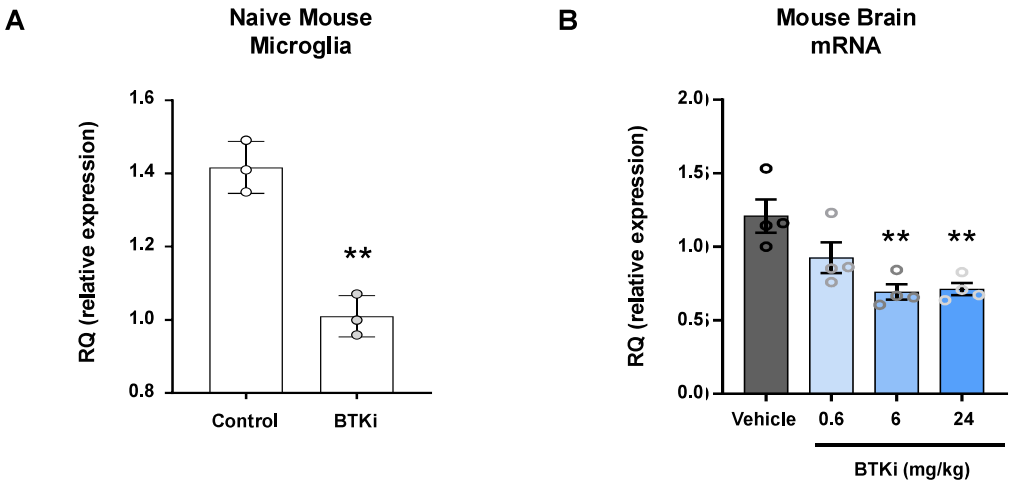
A
Naive Mouse
Microglia
RQ (relative expression)
1.6
1.4
1.2
1.0
0.8
**
Control
BTKi
B
Mouse Brain
mRNA
RQ (relative expression)
2.0
1.5
1.0
0.5
0.0
**
**
Vehicle
0.6
6
24
BTKi (mg/kg)

Fig. S8. mRNA expression of the *Rgs1* gene. (A) Mouse microglia treated with PRN2675. (B) Brain tissue from naïve mice administered a PRN2675 (dosed 1× daily orally for 5 days), compared with vehicle, indicate central pharmacodynamic effect of PRN2675 *in vivo*. RNA isolation from the one-quarter mouse brain was performed with a RNeasy Lipid Tissue Mini Kit (Qiagen, cat# 74804). Brain tissue was homogenized in 1 mL of QIAzol Lysis Reagent with a handheld homogenizer and the RNeasy kit was used per protocol. The RNA quantity was then measured using Nanodrop. cDNA was prepared with the Quantitect Reverse Transcription Kit (Qiagen, cat# 205313); cDNA was stored at −80 °C until use. For quantitative PCR, a master mix solution was prepared with the following volumes: 10 µL Fastlane master mix, 5.3 µL H_2O, 0.5 µL probe (Thermo Scientific, RGS1 Mm00450170_m1), 0.2 µL housekeeping probe 1 (Thermo Scientific, RPL37a: Mm01546394_s1). The master mix was aliquoted into a 384-well PCR plate and 2 µL sample was added to each well. Samples were run in triplicate. P-values are indicated by *≤0.05, **≤0.01, ***≤0.001, and ****≤0.0001. BTKi = Bruton's tyrosine kinase inhibitor; cDNA = complementary DNA; RQ = relative quantification. Source data are provided as a Source Data file.

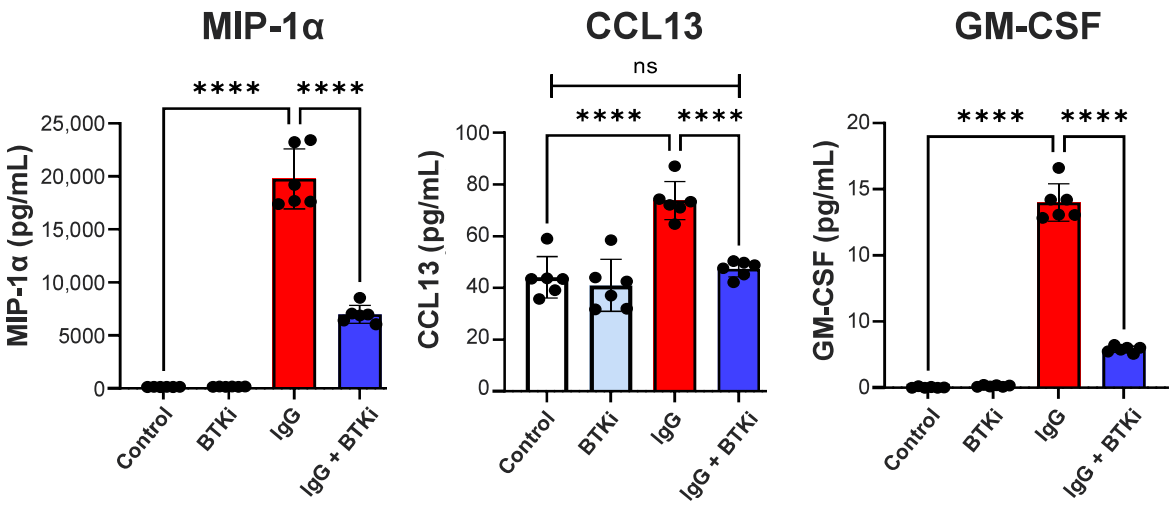
MIP-1α
CCL13
GM-CSF
MIP-1α (pg/mL)
CCL13 (pg/mL)
GM-CSF (pg/mL)
****
****
ns
25,000
20,000
15,000
10,000
5000
0
100
80
60
40
20
20
15
10
10
Control
BTKi
IgG
IgG + BTKi

Fig. S9. Effect of tolebrutinib 100 nM on secretion of MIP-1α, CCL13, and GM-CSF in human iPSC-derived microglia, 24 hours after complexed IgG stimulation. Complexed IgG used was 10 µg/mL Fc OxyBURST™ (Invitrogen, F2902). **** P≤0.0001. P-values were calculated using one-way ANOVA with post hoc Sidak test. CCL = chemokine (C-C motif) ligand; GM-CSF = granulocyte-macrophage colony-stimulating factor; iPSC = induced pluripotent stem cell; IgG = immunoglobulin G; MIP = macrophage inflammatory protein; ns = non-significant. Source data are provided as a Source Data file.

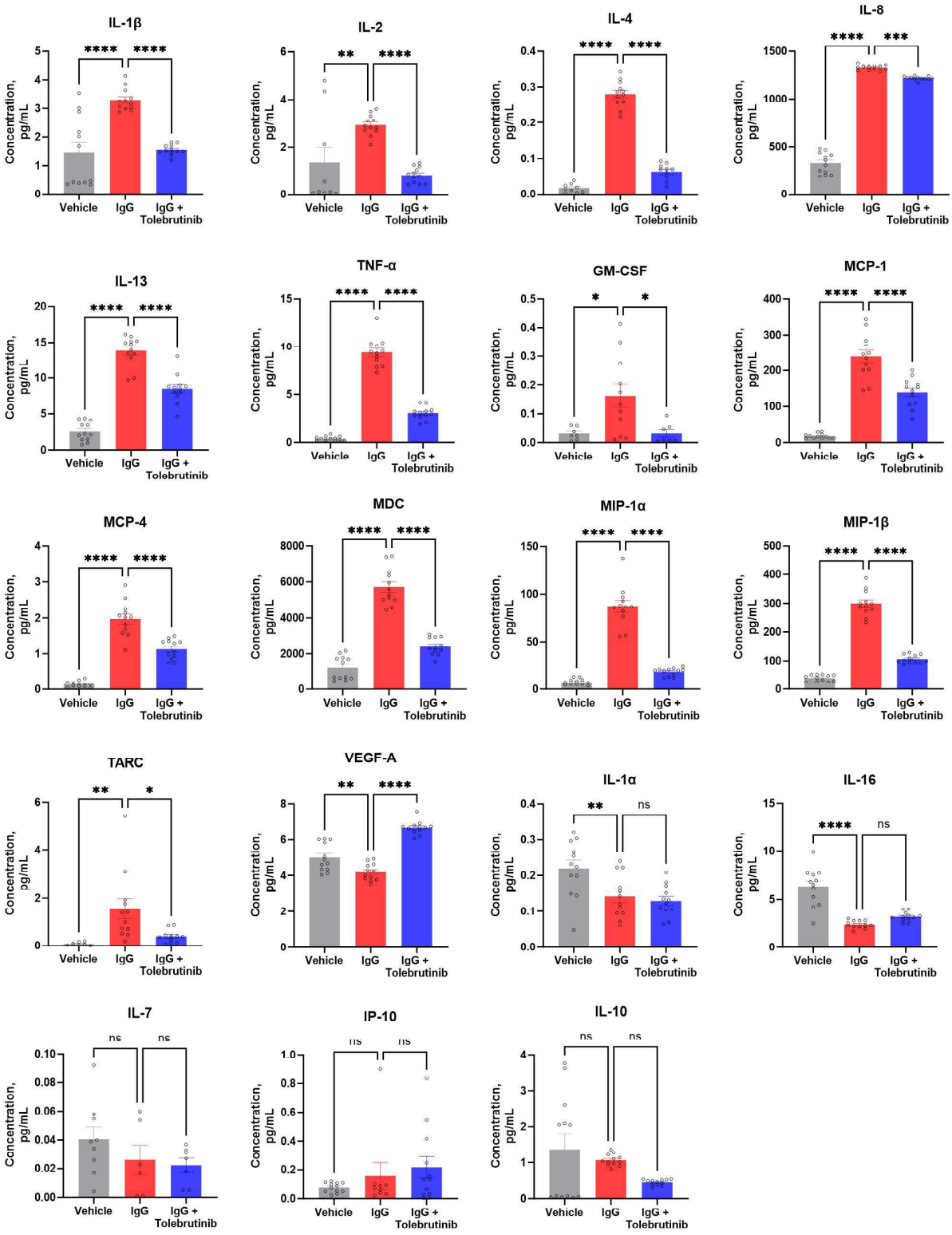
IL-1β
IL-2
IL-4
IL-8
IL-13
TNF-α
GM-CSF
MCP-1
MCP-4
MDC
MIP-1α
MIP-1β
TARC
VEGF-A
IL-1α
IL-16
IL-7
IP-10
IL-10
Concentration, pg/mL
Vehicle
IgG
IgG + Tolebrutinib
ns

Fig. S10. Effect of tolebrutinib 100 nM on cytokine and chemokine secretion in human microglia, when applied after IgG stimulation. Assessments were made using multiplex panels, 24 hours after tolebrutinib and Fc OxyBURST™ (10 µg/mL) administration, which was added 24 hours after Fc OxyBURST™ alone. P-values are indicated by *≤0.05, **≤0.01, ***≤0.001, and ****≤0.0001. IL = interleukin; TNF = tumor necrosis factor; GM-CSF = granulocyte-macrophage colony-stimulating factor; MCP = monocyte chemoattractant protein; MDC = macrophage-derived chemokine; MIP = macrophage inflammatory protein; TARC = thymus and activated-regulated chemokine; VEGF = vascular endothelial growth factor; IP-10 = interferon gamma-induced protein 10. Source data are provided as a Source Data file.

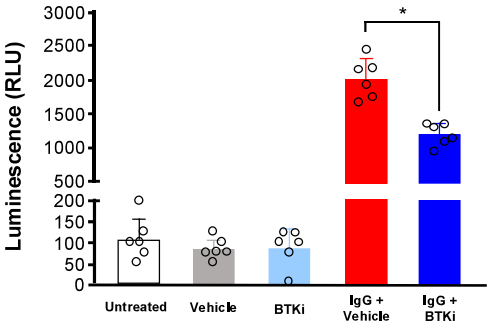
Luminescence (RLU)
3000
2500
2000
1500
1000
500
200
150
100
50
0
*
Untreated
Vehicle
BTKi
IgG + Vehicle
IgG + BTKi

Fig. S11. NF-κB activation in a human monocytic cell line. Effect of tolebrutinib on NF-κB activation in a human monocytic cell line after complexed IgG stimulation. The THP1-Lucia NF-κB monocytic cell line (Invivogen) was stimulated with Fc OxyBURST™ (Invitrogen, F2902) at a concentration of 10 µg/mL in the presence of 1 µM tolebrutinib or DMSO 0.001% (n=6 technical replicates). *P≤0.001 (one-way ANOVA with post hoc Sidak test). DMSO = dimethyl sulfoxide; IgG = immunoglobulin G; NF-κB = nuclear factor-kappa B; RLU = relative light unit. Source data are provided as a Source Data file.

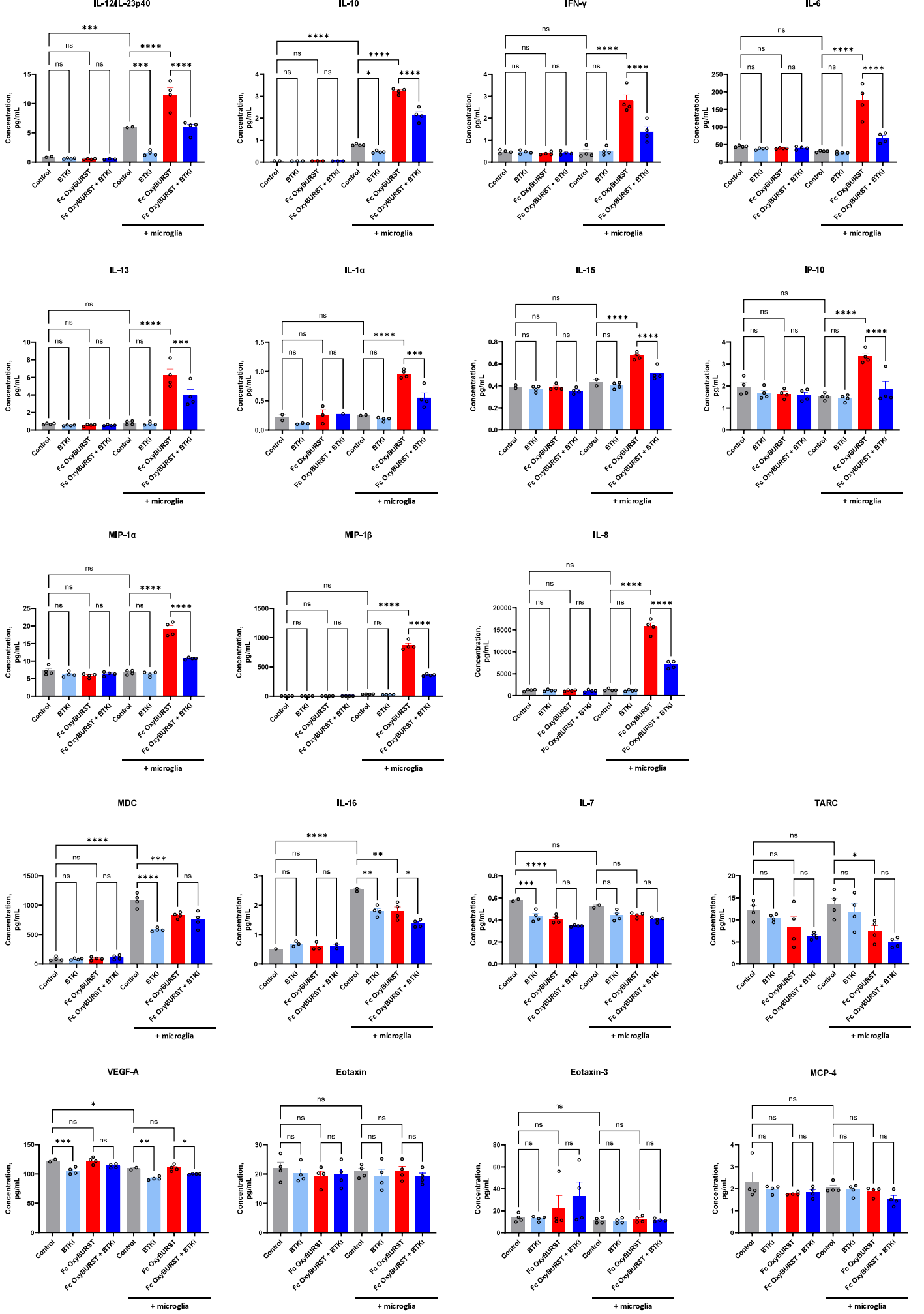
IL-12/IL-23p40
IL-10
IFN-γ
IL-6
IL-13
IL-1α
IL-15
IP-10
MIP-1α
MIP-1β
IL-8
MDC
IL-16
IL-7
TARC
VEGF-A
Eotaxin
Eotaxin-3
MCP-4
Concentration, pg/mL
Control
BTKi
Fc OxyBURST
Fc OxyBURST + BTKi
+ microglia
ns
*
**
***
****

Fig. S12. Effect of tolebrutinib 100 nM on cytokine and chemokine secretion in a human iPSC-derived culture of astrocytes and neurons, with and without microglia. Assessments were made using multiplex panels, 24 hours after IgG, Fc OxyBURST™, stimulation and tolebrutinib addition. P-values are indicated by *≤0.05, **≤0.01, ***≤0.001, and ****≤0.0001. IL = interleukin; IFN = interferon; IP = interferon gamma-induced protein; MIP = macrophage inflammatory protein; MDC = macrophage-derived chemokine; TARC = thymus and activated-regulated chemokine; VEGF = vascular endothelial growth factor; MCP = monocyte chemoattractant protein. Source data are provided as a Source Data file.

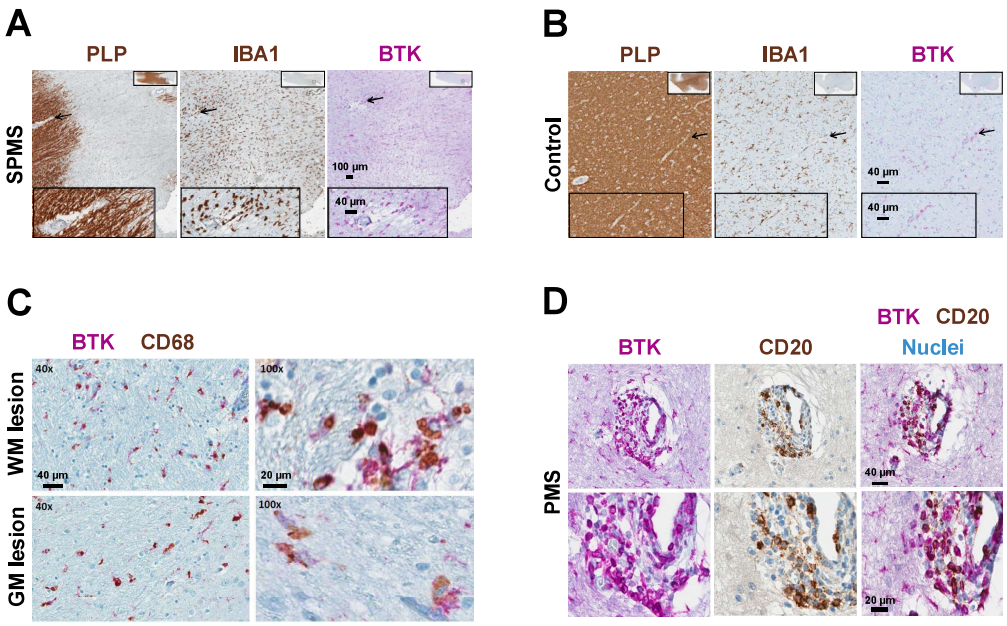
A
PLP
IBA1
BTK
SPMS
100 µm
40 µm
B
PLP
IBA1
BTK
Control
40 µm
40 µm
C
BTK
CD68
WM lesion
GM lesion
40x
100x
40 µm
20 µm
40x
100x
D
BTK
CD20
BTK CD20
Nuclei
PMS
40 µm
20 µm

Fig. S13. (A–B) Immunohistochemistry analysis for myelin PLP, IBA1 and BTK around a lesion rim in an SPMS (Panel A) and a control (Panel B) specimen. (C) Immunohistochemistry analysis for BTK and CD68 in a white and grey matter lesion in a PMS specimen. (D) Immunohistochemistry analysis for BTK and CD20 around a blood vessel in a PMS specimen. $BTK^+/CD20^+$ B cells were present almost exclusively in the perivascular space in progressive MS patient tissue. Positive: BTK (Cell Signaling Technology; Cat# 8547; protein concentration, 5.88 μg/mL; final concentration, 0.29 μg/mL [1:20]); CD20 (Biocare Medical; Cat# CM 004; protein concentration 23.75 μg/mL; final concentration 0.24 μg/mL [1:100]). Negative: rabbit monoclonal IgG (Abcam; Cat# ab172730; protein concentration, 1.89 mg/mL; final concentration, 0.29 μg/mL [1:6500]); mouse IgG2a (BD Pharmingen; Cat# 550339; protein concentration, 250 μg/mL; final concentration, 0.24 μg/mL [1:1050]). Antibodies diluted in 10% Goat serum (Vector Labs) in 0.01% Triton X in phosphate-buffered saline. Tissues: Positive: formalin-fixed, paraffin-embedded (FFPE) human lymph node (Ventana). Reagents for staining: ChromoMap 3,3′-diaminobenzidine (DAB; Roche; Cat# 05266645001); Omni anti-rabbit HRP (Roche; Cat # 05269679001); Omni anti-mouse HRP (Roche; Cat# 05269652001); Discovery Purple (Roche; Cat# 07053983001); Hematoxylin (Roche; Cat# 05266726001); Bluing Solution (Roche; Cat# 05266769001); Discovery Inhibitor (Roche; Cat# 07017944001). BTK = Bruton's tyrosine kinase; CD = cluster of differentiation; GM = grey matter; HRP = horseradish peroxidase; IBA1 = ionized calcium binding adaptor molecule 1; MS = multiple sclerosis; PLP = proteolipid protein; PMS = progressive MS; SPMS = secondary progressive MS; WM = white matter.

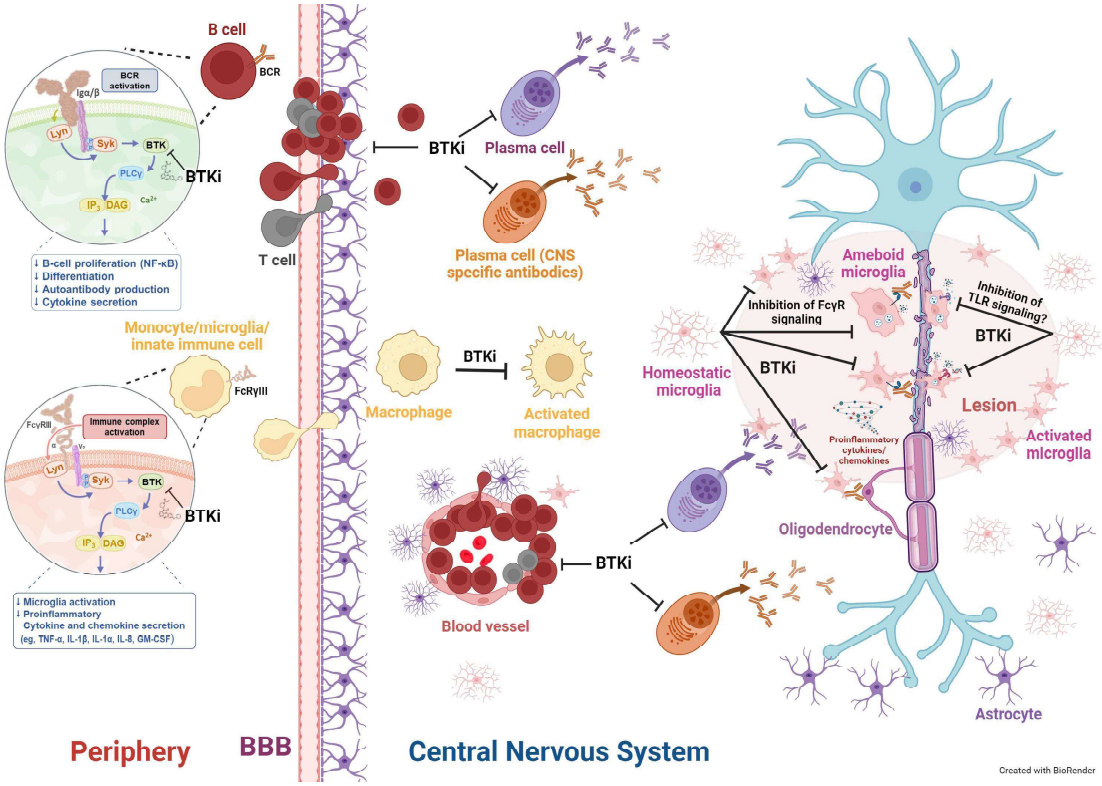
B cell
BCR
BCR activation
Igα/β
Lyn
Syk
BTK
PLCγ
IP3
DAG
Ca2+
BTKi
↓ B-cell proliferation (NF-κB)
↓ Differentiation
↓ Autoantibody production
↓ Cytokine secretion
T cell
BTKi
Plasma cell
Plasma cell (CNS specific antibodies)
Monocyte/microglia/ innate immune cell
FcRγIII
FcγRIII
Immune complex activation
BTKi
↓ Microglia activation
↓ Proinflammatory Cytokine and chemokine secretion (eg, TNF-α, IL-1β, IL-1α, IL-8, GM-CSF)
BTKi
Macrophage
Activated macrophage
BTKi
Blood vessel
Ameboid microglia
Inhibition of FcγR signaling
Inhibition of TLR signaling?
BTKi
BTKi
Homeostatic microglia
Lesion
Activated microglia
Proinflammatory cytokines/ chemokines
Oligodendrocyte
Astrocyte
Periphery
BBB
Central Nervous System
Created with BioRender

Fig. S14. Proposed mechanisms of BTKi in MS. A brain penetrant BTKi, has the potential to target adaptive and innate immunopathological mechanisms of MS on both sides of the BBB. BTK is located downstream of the BCR in B cells, and immunoglobulin receptors (e.g., FcγR) and molecular pattern sensors (e.g., TLRs) in innate immune cells, including monocytes, macrophages, and CNS-resident microglia. In MS, BTKi-induced blockade of BCR signaling in the periphery and the CNS may suppress B-cell proliferation, differentiation of B cells into plasma cells, and autoantibody and cytokine production, resulting in decreased CNS lymphocytic infiltration and neuroinflammation (reviewed in Krämer, J., et al[13]). BTKi-induced blockade of pathogenic innate immune cell signaling is proposed to decrease cytokine production and the activation of macrophages and microglia in the CNS, potentially suppressing immune-mediated demyelination and axonal damage. BBB = blood-brain barrier; BCR = B-cell receptor; BTK = Bruton's tyrosine kinase; BTKi = BTK inhibitor; CNS = central nervous system; DAG = diacylglycerol; FcγR = Fc-gamma receptor; IL = interleukin; IP3= inositol 1,4,5-trisphosphate; NF-κB = nuclear factor-kappa B; PLCγ = phospholipase C gamma; Syk = spleen tyrosine kinase; TLR = Toll-like receptor; TNF-α = tumor necrosis factor-alpha. Created in BioRender. Gruber, R. (2023) https://BioRender.com/j66p849.

A

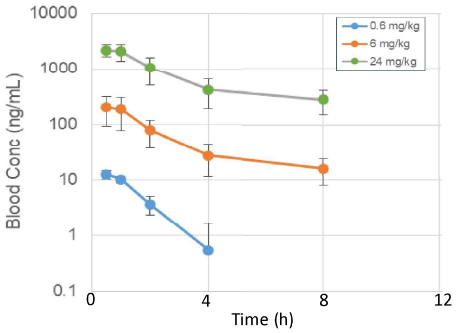

Treatment Groups	Animals per group
Vehicle	4
PRN2675 0.6 mg/kg	4
PRN2675 6.0 mg/kg	4
PRN2675 24 mg/kg	4

*Mice were perfused

Dose	Brain (ng/g)	Blood (ng/mL)	Brain / Blood
0.6 mg/kg QD	2.71	10	0.271
6 mg/kg QD	113	423	0.267
24 mg/kg QD	851	1910	0.446

1hr post dose

B

Target IC50 (nM)

	Tolebrutinib	PRN2675
BTK	0.7	1.2
BLK	0.6	4
BMX	1.1	3.8
EGFR	4.1	31
ERBB2	60	6.2
ERBB4	1	4200
ITK	365	>5000
JAK3	1851	>5000
TEC	1	1.6
TXK	1.7	15.6

Fig. S15. PRN2675 brain penetrance and pharmacokinetics in mouse and kinase selectivity. (A) Time course of PRN2675 blood concentration following PO dosing and brain exposure 1 hour post dose. (B) Kinase selectivity for BTK inhibitors tolebrutinib and PRN2675. IC_{50} = half maximal inhibitory concentration. Source data are provided as a Source Data file.

SUPPLEMENTARY TABLES

Table S1. Samples for *in vitro* investigation of the mouse transcriptomic signature

Samples ID	**Time point**	**New ID**
10042018 No Tx-1	24 hours	13
10042018 No Tx-2	24 hours	14
10042018 No Tx-3	24 hours	15
10042018 No Tx-4	24 hours	16
10042018 Agg IgG-1	24 hours	17
10042018 Agg IgG-2	24 hours	18
10042018 Agg IgG-3	24 hours	19
10042018 Agg IgG-4	24 hours	20
10042018 Agg IgG + PRN-1	24 hours	21
10042018 Agg IgG + PRN-2	24 hours	22
10042018 Agg IgG + PRN-3	24 hours	23
10042018 Agg IgG + PRN-4	24 hours	24

Table S2. Human autopsy samples

Patient samples							
Sample #	**Sample ID**	**Sample source**	**Sample type**	**PMI**	**RNAseq**	**Protein quantification**	**IHC**
1	5293	UCLA BB	CTL/Liver failure, pneumonia	11.5	X	X	
2	4823	UCLA BB	CTL/Lennox Gastaut syndrome, pneumonia aspiration	11.8	X	X	
3	5214	UCLA BB	CTL, Normal	19.5	X	X	
4	4621	UCLA BB	CTL, Breast, uterine and colon cancer	17.6	X	X	
5	4514	UCLA BB	CTL, Lung cancer, COPD	17.3	X	X	

6	5154	UCLA BB	RRMS	12.6	X	X	
7	5139	UCLA BB	RRMS	36.8	X	X	
8	5095	UCLA BB	RRMS	8.1	X	X	
9	5102	UCLA BB	RRMS	14.7	X	X	
10	5123	UCLA BB	RRMS	24.8	X	X	
11	5053	UCLA BB	SPMS	24.9	X	X	
12	5056	UCLA BB	SPMS	20.1	X	X	
13	5276	UCLA BB	SPMS	16.9	X	X	
14	4959	UCLA BB	SPMS	21.1	X	X	

15	4678	UCLA BB	SPMS	13.6	X	X	
16	5252	UCLA BB	SPMS	10.5	X	X	
17	4961	UCLA BB	PPMS	9.3	X	X	
18	4951	UCLA BB	PPMS	24.8	X	X	
19	2485	UCLA BB	PPMS	9	X	X	
20	5149	UCLA BB	PPMS	11	X	X	
21	3816	UCLA BB	PPMS	20.7	X	X	
22	MS-20-9	CC RAP	PPMS				X
23	MS-32-11-2	CC RAP	PPMS				X

24	MS-45-13-1	CC RAP	PPMS				X
25	MS-22-10-1	CC RAP	PPMS				X
26	MS-138-8-3	CC RAP	SPMS				X
27	MS-117-9-2	CC RAP	SPMS				X
28	MS-151-5-1	CC RAP	SPMS				X
29	MS-85-4-1	CC RAP	RRMS				X
30	MS-19-7-1	CC RAP	RRMS				X
31	A168-3-5	CC RAP	CTL, diabetes, chronic kidney disease, myocardial infarction				X

32	A119-3-2	CC RAP	CTL				X

UCLA Brain Bank (UCLA BB), Cleveland Clinic Rapid Autopsy Program (CC RAP)

Percentage female among sample types: Control (66.7), RRMS (42.9), SPMS (57.1), PPMS (44.4)

Age of sample donors (mean, standard deviation): Control (59.0, 17.9), RRMS (64.3, 11.6), SPMS (52, 10.1), PPMS (55.2, 8.5)